Ultrasound in Med. & Biol., Vol. 44, No. 10, pp. 2105–2114, 2018

0301-5629/$ - see front matter

https://doi.org/10.1016/j.ultrasmedbio.2018.05.025

● *Original Contribution*

REACTIVE OXYGEN SPECIES MEDIATE THERAPEUTIC ULTRASOUND-INDUCED, MITOGEN-ACTIVATED PROTEIN KINASE ACTIVATION IN C28/I2 CHONDROCYTES

HARMANPREET KAUR,* ARNO G. SIRAKI,† MONIKA SHARMA,‡ HASAN ULUDAĞ,§ DOUGLAS N. DEDERICH,* PATRICK FLOOD,* and TAREK EL-BIALY*

* Department of Dentistry, University of Alberta, Edmonton, Alberta, Canada; † Faculty of Pharmacy and Pharmaceutical Sciences, University of Alberta, Edmonton, Alberta, Canada; ‡ Department of Medical Microbiology and Immunology, University of Alberta, Edmonton, Alberta, Canada; and § Department of Chemical and Material Engineering, University of Alberta, Edmonton, Alberta, Canada

(*Received* 7 *January* 2018; *revised* 3 *April* 2018; *in final from* 29 *May* 2018)

Abstract—Low-intensity pulsed ultrasound (LIPUS) has been used for the treatment of non-healing fractures because of its therapeutic properties of stimulating enhancing endochondral bone formation. However, its mechanism of action remains unclear. In this study, we hypothesized that LIPUS activates mitogen-activated protein kinases through generation of reactive oxygen species. C28/I2 cells were stimulated with LIPUS for 10 and 20 min, while the control group was treated using a sham LIPUS transducer. Through quantitative reverse transcription polymerase chain reaction and immunoblot analyses, we determined that LIPUS application increased reactive oxygen species generation and cell viability in C28/I2 cells. There were increases in the phosphorylation level of ERK1/2 and in expression of *SOX9, COL2 A1* and *ACAN* genes. These effects were reversed when cells were treated with diphenylene iodonium, which is known to inhibit NADPH oxidase. It was concluded that exposure of chondrocytes to LIPUS led to reactive oxygen species generation, which activated MAPK signaling and further increased chondrocyte-specific gene markers involved in chondrocyte differentiation and extracellular matrix formation. (E-mail: kaur3@ualberta.ca) © **2018 World Federation for Ultrasound in Medicine & Biology. All rights reserved.**

KeyWords: **Reactive oxygen species, Superoxide, Chondrocytes, Low-intensity pulsed ultrasound.**

INTRODUCTION

Cartilage is an avascular tissue that has little capacity for self-repair. Chondrocytes play an important role in cartilage maintenance and endochondral ossification. These are mechanosensitive cells present in the cartilage that synthesize and maintain its extracellular matrix (ECM). These cells are surrounded by an abundant ECM containing collagen and proteoglycan. Chondrocytes also participate in bone formation *via* the endochondral ossification process. In endochondral ossification, the chondrocytes undergo a chronologic process of differentiation leading to formation of cartilage, which acts as a scaffold that is replaced by bone. Mechanical loading of chondrocytes is important for growth and maintenance of cartilage and leads to an increase in expression of the ECM genes (Whitney et al. 2012). Loading within physiologic limits has an anabolic effect on the cells, whereas either an excess or an absence of mechanical load leads to cartilage destruction. Studies found that reduced mechanical loading, as in animals fed a soft diet (Fanghänel and Gedrange 2007) or artificially immobilized (Jortikka et al. 1997), led to reduced compressive load, which affected not only the cartilage but also the underlying subchondral bone (Sato et al. 2005).

Low-intensity pulsed ultrasound (LIPUS) is a form of acoustic wave that produces micromechanical strain in the tissue through which it passes, leading to specific biochemical events (Tanaka et al. 2015). In recent years, LIPUS stimulation has been employed to exert an anabolic effect on osteoblasts and on bone formation (Busse et al. 2009) and to enhance new blood vessel formation in wound healing and bone fracture sites (Cheung et al. 2011). LIPUS enhanced the expression of genes involved in cartilage matrix production, such as

Address correspondence to: Harmanpreet Kaur, 7-020, Katz Group Centre for Pharmacy and Health Research, University of Alberta, Edmonton, AB, Canada T6G 2E1. E-mail: kaur3@ualberta.ca

Conflicts of Interest: The authors have no conflicts of interest and no competing financial interests.

SOX9, COL2 A1, and *ACAN*, and stimulated chondrogenesis (Hasanova et al. 2011). Because of its stimulatory effect on bone healing, LIPUS has been approved by the U.S. Food and Drug Administration and Health Canada for treatment of delayed and non-union bone fracture. LIPUS has chondrogenic properties and has also been proposed for the treatment of early-stage osteoarthritis (Cheng et al. 2014).

The exact mechanism underlying the beneficial effects of LIPUS on cartilage matrix production is still not fully understood. Mechanical stimulation by LIPUS has been reported to enhance integrin expression (Sato et al. 2014), increase phosphoinositide 3-kinase activation (Takeuchi et al. 2008), enhance actin polymerization (Uddin et al. 2013) and increase mitogen-activated protein kinase (MAPK) signaling (Kusuyama et al. 2014). MAPKs play an important role in various cellular processes such as cell growth, differentiation, survival and apoptosis. This multifunctional signaling pathway consists of three classes of serine/threonine kinases: extracellular signal regulated kinase 1/2 (ERK1/2), p38 and c-Jun N-terminal kinase (JNK). ERK1/2 is activated mainly by growth factors and mediates cell proliferation and differentiation; p38 and JNK are activated mainly by external stresses in the form of physical and chemical stimulation (Fujisawa et al. 2007). MAPK activation is a three-step process consisting of phosphorylation of MAP 3-K, which then activates and phosphorylates MAP 2-K and increases the activity of one or more MAPKs (*i.e.,* ERK1/2, p38 and JNK). MAPK phosphatase (MKP) enzyme dephosphorylates and deactivates the MAPK pathway (Boutros et al. 2008; Plotnikov et al. 2011; Son et al. 2013) .

Studies in the last decade have indicated that MAPKs are regulated by the oxidation−reduction reactions that produce ROS such as superoxide ($O^{2\bullet-}$), hydrogen peroxide (H_2O_2) and hydroxyl radical ($\bullet OH$). ROS are intracellular second messengers in cell signaling as they are promptly generated, extremely diffusible, effortlessly metabolized and present in all cell types (Sauer et al. 2001). The chief source of ROS in the cell is the electron transport chain in mitochondria. However, because of the presence of mitochondrial superoxide dismutase, superoxide levels are kept at a low level. Another source of ROS is NADPH oxidases (NOX), which are a group of seven plasma membrane-bound enzymes NOX1−NOX5 and DUOX1 and DUOX2. NOX2 is the prototype of NOX enzyme, and NOX1, NOX3 and NOX4 are closely related to NOX2; NOX4 is only 39% similar to NOX2. The main target of ROS in MAPK regulation is protein tyrosine phosphatase (PTP), which contains a cysteine residue in its active site. ROS induces oxidative modification of the active site cysteine by the formation of a disulfide bond (−S−S) causing inactivation of PTP and thereby increasing phosphorylation by tyrosine kinase (Son et al. 2013). Previous studies have reported nitric oxide (NO) generation by LIPUS in osteoblasts (Reher et al. 2002) and in endothelial cells (Hsu and Huang 2004), but there are no reports of ROS generated by LIPUS.

In the present study, we hypothesized that LIPUS application affects ROS levels in chondrocytes and activates the MAPK pathway. To investigate this hypothesis, we used the C28/I2 human chondrocyte cell model and investigated intracellular signaling involving MAPK, as well as expression of genes affecting extracellular matrix turnover (*SOX9, ACAN* and *COL2 A1*).

METHODS

Materials

The C28/I2 human chondrocyte cell line was a kind gift from Dr. Mary Goldring (Hospital for Special Surgery, Weill Medical College, Cornell University, New York, NY, USA); Dulbecco's modified Eagle's medium F12 (DMEM F12) with L-glutamine and 4-(2-hydroxyethyl)-1-piperazineethanesulfonic acid (HEPES), fetal bovine serum (FBS), Dulbecco's phosphate-buffered saline (DPBS) and Hanks' balanced salt solution (HBSS) were purchased from Life technologies (Grand Island, NY, USA). Penicillin and streptomycin were purchased from Hyclone GE (Logan, UT, USA). Dihydroethidine (DHE), diphenyleneiodonium (DPI), MTT [(3-(4, 5-dimethylthiazol−2-yl)-2, 5- diphenyl tetrazolium bromide], chloroform, isopropanol, bovine serum albumin (BSA) and dimethyl sulfoxide (DMSO) were purchased from Sigma Aldrich (St Louis, MO, USA). Sodium dodecyl sulfate (SDS), polyacrylamide and nitrocellulose membrane were purchased from Bio-Rad (Tokyo, Japan). A high-capacity reverse transcription kit for cDNA preparation was purchased from Applied Biosystems (Foster City, CA, USA). Antibodies that were used in immunoblot analysis (anti-ERK1/2, anti-phospho-ERK1/2, anti-p38, anti-phospho-p38, anti -JNK, anti-phospho-JNK and horseradish peroxidase-conjugated anti-IgG) were purchased from Cell Signaling Technology (Danvers, MA, USA). A Pierce BCA protein assay kit, Pierce protease inhibitor and 0.05% trypsin−EDTA solution were purchased from ThermoFisher (Rockford, IL, USA). An enhanced chemiluminescence (ECL) Western blot reagent kit was purchased from Amersham GE Health Care (Buckinghamshire, UK).

Cell culture

C28/I2 human chondrocytes (1.5×10^5 /mL) were cultured in six-well plates in medium containing DMEM/F12, 10% FBS and 50 units/mL penicillin and 50μg/mL of streptomycin. Cells were incubated at 37°C

in a humid chamber with 5% CO_2 and cultured for 24 h until the first LIPUS application. The cells were washed twice with DPBS and harvested after 1, 3, 6, 12 and 24 h of LIPUS. For ROS inhibition, cells were cultured at the exact same cell density and conditions. Before addition of DPI, cells were starved by replacing the medium containing FBS with basal medium (DMEM/F12 without FBS, penicillin and streptomycin). DPI was added to DMEM/F12 at least 1 h before LIPUS application. The cells were washed with pre-warmed PBS and harvested using 0.05% trypsin−EDTA solution. All experiments were performed in triplicate.

LIPUS stimulation

Cells were exposed to 10 and 20 min of LIPUS; the control group was treated with a sham LIPUS transducer. The LIPUS device was custom-made and provided by SmileSonica Inc. (Edmonton, AB, Canada). The device generated a 200-μs burst of 1.5-MHz sine waves with a repetition rate of 1 kHz and spatial averaged intensity of 30 mW/cm^2. These parameters have been used in our lab in the past (El-Bialy et al. 2010; Kaur et al. 2017a, 2017b). The six-well plates were placed on the surface of the transducers. The coupling gel (SmileSonica) was applied between the LIPUS transducer and the base of the six-well plates for the transmission of ultrasound waves. Based on LIPUS application and DPI addition, the groups were control DPI(−), not exposed to LIPUS or DPI; LIPUS 10 min DPI(−), exposed to 10 min of LIPUS and no DPI; LIPUS 20 min DPI(−), exposed to 20 min of LIPUS and no DPI; control DPI(+), not exposed to LIPUS but containing DPI; LIPUS 10 min DPI(+), exposed to 10 min of LIPUS in the presence of DPI; and LIPUS 20 min DPI(+), exposed to 20 min of LIPUS in the presence of DPI.

DHE fluorescence assay

The cells were washed with pre-warmed (37˚C) DPBS solution and suspended in DMEM/F12 (without phenol red) at a concentration of 1×10^5 cells/ mL in the presence or absence of DPI (10 μM). The suspended cells were incubated with DHE (25 μM) for 20 min in an incubator before LIPUS application. Cells were sonicated with LIPUS according to their group, and 100 μL of cell suspension was collected from each sample in triplicate at 0, 15, 30, 45, 60, 90 and 120 min and were dispensed onto a 96-well ViewPlate with black well walls. Fluorescence intensity was quantified using a Tecan M2000 microplate reader (Tecan Infinite M200, Durham, NC, USA) with excitation and emission wavelengths of 480 and 570 nm, respectively, at room temperature.

Cell viability assay

The cells were seeded on 6-well plate in the presence and absence of DPI, and the readings were taken after 24 h of LIPUS. The MTT assay was used as a measure of cell viability. Eight hundred microliters of MTT solution (dissolved in HBSS using a concentration of 5 mg/mL) was added to each well containing 2 mL of the medium and incubated for 2 h at 37˚C. The medium was replaced with 2 mL of pure DMSO (≥ 99.9%) to dissolve MTT formazan crystals. Absorbance was measured at 570 nm using the Tecan M2000 microplate reader at room temperature.

Quantitative real-time reverse transcription polymerase chain reaction

TRIzol reagent was used according to the manufacturer's instructions to prepare total RNA. RNA concentration was measured using a NanoDrop 2000C spectrophotometer (Thermo Fisher, Wilmington, DE, USA). cDNA was synthesized from 1 μg total RNA using the High-Capacity cDNA Reverse Transcriptase kit according to the instructions in the reaction volume of 20 μL. After reverse transcription reaction, 1 of 10 dilutions were made from the template to be used in real-time PCR. Ten microliters of the real-time reaction mixture consisting of 3 μL of cDNA, 1 μL each of forward and reverse primers and 5 μL of the master mix containing SYBR green dye. The mixtures were heated at 95˚C for 2 min before going through 40 cycles of the denaturation step (15 s at 95˚C) and an annealing step (1 min at 60˚C) using the 7500 Real-Time PCR system during which data were collected. Glyceraldehyde-3-phosphate dehydrogenase (GAPDH) was used as an internal control in each run. Normalized fluorescence was plotted against cycle number (amplification plot), and the threshold suggested by the software was used to calculate C_t (cycle at threshold). $\Delta\Delta C_t$ analysis was used to determine the differences in gene expression compared with the control. (Primer sequences used in this study are listed in Supplementary Table S1 [online only].)

Immunoblotting

For Western blotting analysis, the cells were cultured for 1, 3, 6, 12 and 24 h after a single ultrasound exposure. The cells were then washed with cold PBS twice and lysed on ice for 30 min in RIPA buffer (50 mM Tris, pH 8.0, 150 mM NaCl and 1%Nonidet P-40) and freshly added 10^{-6} M protease inhibitor (Pierce protease inhibitor, Thermo Fisher). The lysates were used as samples after centrifugation (10,000 rpm for 10 min at 4˚C). Total protein concentration was determined using the Pierce BCA kit, and SDS−polyacrylamide gel electrophoresis was performed on 25 μg of

each protein. After SDS-polyacrylamide gel electrophoresis, proteins were transferred onto a nitrocellulose membrane. The membrane was blocked for 1 h at room temperature with 5% BSA in 1% Tris-buffered saline−Tween and incubated overnight at 4˚C with primary antibody (total ERK1/2, phosphor ERK1/2, total p38, phosphor p38, total JNK and phosphor JNK), diluted 1 to 1000 with 5% BSA in 1% Tris-buffered saline−Tween. After incubation with HRP-conjugated anti-rabbit IgG (1:3000) for 1 h at room temperature, the blots were detected with Amersham ECL Western Blotting detection reagent, visualized using the ChemiDoc MP Gel imaging system (Universal Hood III, Bio-Rad, Hercules, CA, USA) and quantified using ImageJ software (National Institutes of Health, Bethesda, MD, USA).

Statistical analysis

Data were summarized as the mean ± standard deviation where error bars represent standard deviations. Two statistical tests were applied: (i) A two-way repeated-measure analysis of variance followed by the Bonferroni *post hoc* test was used to determine the significance for treatment and time. (ii) To study the effect of DPI at each time point, a one-way analysis of variance followed by the Bonferroni *post hoc* test was used. The level of significance was set at $p < 0.05$.

RESULTS

Effect of LIPUS on ROS generation

In non-DPI-treated groups, LIPUS caused a statistically significant increase in ROS generation compared with control DPI(−) ($p < 0.05$), indicating the ability of LIPUS to increase ROS levels. From 30 min onward, the LIPUS 10 min DPI(−) group exhibited statistically different increased ROS levels compared with the other groups. Levels of ROS were reduced in LIPUS-treated DPI(+) groups (both 10 and 20 min) compared with DPI (−) groups, indicating active quenching of the ROS by DPI (Fig. 1).

LIPUS effect on C28/I2 cell viability

We speculated that the amount of ROS generated by LIPUS stimulation is non-toxic to the cells. Thus, we tested the effect of LIPUS on cell viability in the presence and absence of DPI. After 1 d of LIPUS application, there was a significant increase in cell viability in the DPI(−) group treated with LIPUS 10 min compared with other groups ($p < 0.05$). There was no significant difference between the control and DPI(−) LIPUS 20 min group ($p = 0.078$). There was a significant decrease in cell viability in DPI-treated groups compared with non-DPI-treated groups (Fig. 2).

Effect of LIPUS on NOX2 and NOX4 gene expression

To determine whether LIPUS stimulation increased expression of NOX2 and NOX4, C28/I2 chondrocytes

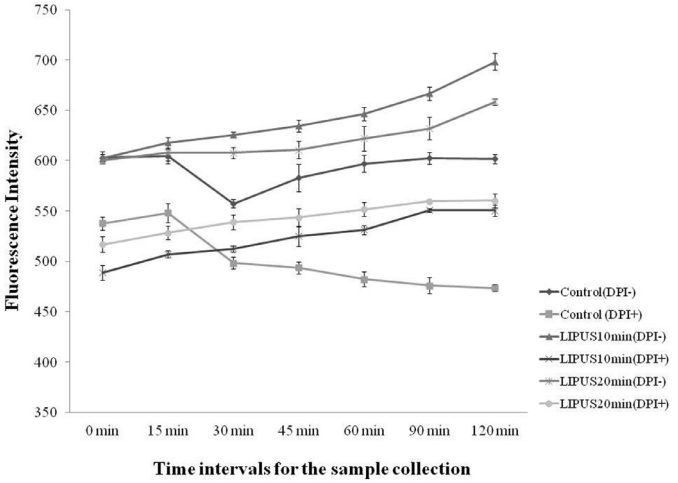

Fig. 1. Effect of LIPUS stimulation on reactive oxygen species generation. C28/I2 chondrocytes were suspended in Dulbecco's modified Eagle's medium/F12 (without phenol red) at a concentration of 1×10^5 cells/mL and incubated with dihydroethidine (25 μM). For reactive oxygen species inhibition, DPI (10 μM) was added to the cell suspension before dihydroethidine. The cells were treated with LIPUS and the samples were collected at 0, 15, 30, 45, 60, 90 and 120 min after LIPUS application. The line graph depicts dihydroethidine fluorescence. LIPUS application resulted in a significant increase in reactive oxygen species generation from 30 min onward; DPI-treated groups exhibited a significant reduction in reactive oxygen species generation. DPI = diphenyleneiodonium; LIPUS = low-intensity pulsed ultrasound.

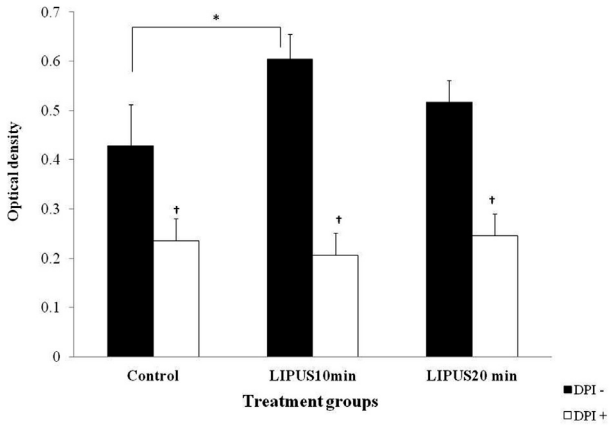

Fig. 2. Detection of C28/I2 chondrocyte cell viability after LIPUS application using the MTT absorbance assay. After 24 h of LIPUS in the presence and absence of DPI (10 μM), the chondrocytes were incubated in MTT solution (5 mg/mL) for 2 h. The formazan crystals formed were dissolved in Dulbecco's modified Eagle's medium, and absorbance was measured. The bar graph depicts the values as the mean ± standard deviation. LIPUS stimulation resulted in a significant increase in cell viability compared with control; DPI-treated group exhibited a significant decrease in cell viability. $^{*}p < 0.05$, $^{\dagger}p < 0.05$ between the corresponding DPI-treated and non-DPI-treated groups. DPI = diphenyleneiodonium; LIPUS = low-intensity pulsed ultrasound.

were stimulated with LIPUS in the presence or absence of DPI, and samples were collected 1, 3, 6, 12 and 24 h after LIPUS application. In non-DPI-treated groups, LIPUS caused a significant increase in *NOX2* mRNA expression at 1, 12 and 24 h, whereas in DPI-treated groups LIPUS increased *NOX2* gene expression at 1 and 12 h (Fig. 3). There were no significant effects of LIPUS on *NOX4* gene expression except at 3 h (Supplementary Fig. S1, online only).

To study the effect of LIPUS on C28/I2 chondrocytes in the presence or absence of DPI, gene expression of chondrocyte-specific markers (*SOX9, ACAN* and *COL2 A1*) were analyzed. *SOX9* expression was significantly higher at 6 h in non-DPI-treated, LIPUS-exposed groups compared with the control group. *SOX9* expression was higher at 1 h in DPI-treated, LIPUS 20 min group compared with the control group; the level of expression level at later time points (Fig. 4A–C). Expression of *ACAN* and *COL2 A1* mRNA was higher in non-DPI-treated, LIPUS-exposed groups at 12 and 24 h. There were no significant changes in DPI-treated groups at any time points in the case of *ACAN* mRNA expression (Fig. 4D–F). For *COL2 A1* expression, LIPUS-exposed, DPI-treated group had a significant increase at 24 h (Fig. 4G–I). (Expression of *SOX9, ACAN* and *COL2 A1* at other time points is illustrated in Supplementary Fig. S2A–F.)

MAPK activation with LIPUS stimulation

To examine the effect of LIPUS application and ROS generation on MAPK phosphorylation, cells were stimulated with LIPUS in the presence and absence of DPI. ERK1/2 phosphorylation was significantly increased 6 and 12 h after LIPUS application while in DPI treated groups, there was significant reduction in ERK1/2 phosphorylation after 1 h and further reductions at later time points (Fig. 5). On the other hand, p38 and JNK phosphorylation exhibited no significant changes at all time points studied in both DPI treated and non-DPI-treated groups (Supplementary Figs. S3 and S4, online only).

DISCUSSION

Low-intensity pulsed ultrasound is a mechanical wave that triggers intracellular signaling in the cell (mechanotransduction), but the mechanism by which LIPUS generates intracellular signals is still unclear. Many intracellular signaling pathways like integrin, stretch-activated ion channels and calcium signaling have been extensively characterized in the context of LIPUS (Choi et al. 2007; Mortimer and Dyson 1988). In this study, we investigated the effect of ROS generated by LIPUS on immortalized human chondrocyte cell proliferation and activation of the MAPK signaling pathway. We hypothesized that LIPUS stimulates chondrocyte viability, increased mRNA expression of *SOX9, ACAN* and *COL2 A1* and activation of MAPK signaling.

To study the effect of LIPUS on ROS generation, we used DHE, a superoxide-specific indicator that is a blue fluorescent dye in the cytosol. In the presence of superoxide, DHE becomes oxidized, generates red fluorescent hydroxyethidium and intercalates with cellular DNA (Peshavariya et al. 2007). Our study found an increase in fluorescence with LIPUS 10 min application followed by LIPUS 20 min. Despite the presence of fluorescence intensity at 0 min, the difference was not significant in the DPI(−) groups (*i.e.,* control DPI(−), LIPUS 10 min DPI(−) and LIPUS 20 min DPI(−)), whereas the difference was significant in the DPI(+) groups (*i.e.,* control DPI(+), LIPUS 10 min DPI(+) and LIPUS 20 min DPI (+)). This could have occurred because the fluorescence intensities of ROS generated in DPI(−) groups were too close to be detected by the plate reader. Meanwhile in the DPI (+) groups, despite the presence of DPI, LIPUS resulted in generation of a small amount of ROS that were detected by the plate reader. In future studies, use of the electron paramagnetic resonance method is recommended for detection of ROS generation. Because DHE is a superoxide-specific indicator, our study illustrated that the ROS generated after LIPUS application are superoxide. For ROS inhibition, we used DPI, which

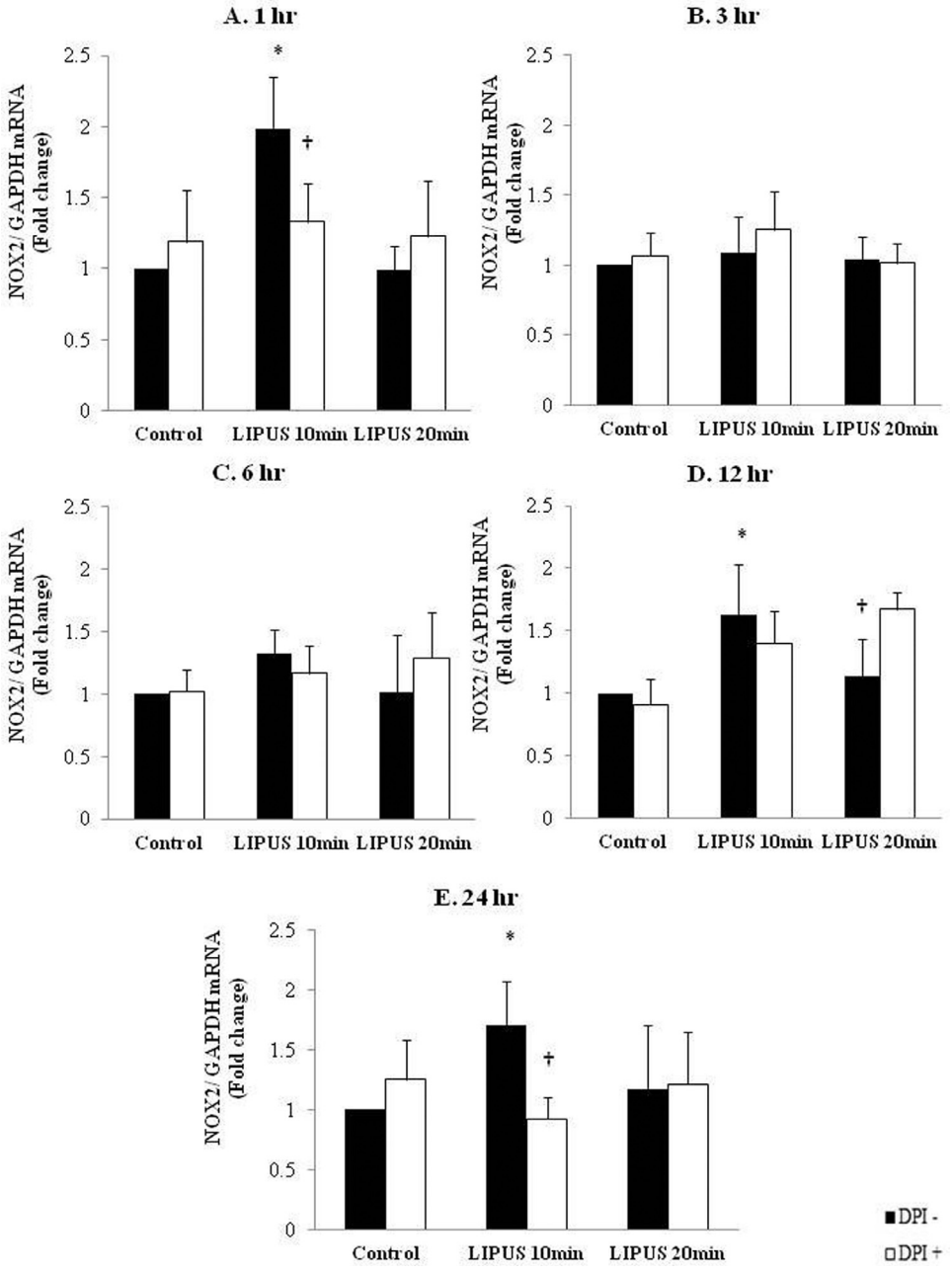

Fig. 3. NOX2 mRNA expression quantified using quantitative real-time reverse transcription polymerase chain reaction in C28/I2 chondrocytes after LIPUS application in the presence or absence of DPI (10 μM). The samples were collected after (A) 1, (B) 3, (C) 6, (D) 12 and (E) 24 h of LIPUS. The bar graph depicts a significant increase in NOX2 mRNA expression after 1 h of LIPUS in the non-treated group, whereas there was a significant increase at 12 h in the DPI-treated group. *$p < 0.05$, $^{\dagger}p < 0.05$ between the corresponding DPI-treated and non-DPI-treated groups. DPI = diphenyleneiodonium; LIPUS = low-intensity pulsed ultrasound.

is most commonly used as a NOX inhibitor. DPI is a flavoprotein oxidoreductase inhibitor that forms phenol radical which attack the flavin adenine dinucleotide (FAD) of the NOX enzyme (Li et al. 2003). There was a significant reduction in superoxide generation in the DPI-treated groups exposed to LIPUS for 10 and 20 min. Because ROS generation is related to oxidative stress, which could affect cell viability, the MTT cell viability assay was carried out to check for ROS toxicity. A significant stimulatory effect of LIPUS treatment on chondrocyte cell viability was observed in the MTT assay, especially in the non-DPI-treated group exposed to LIPUS for 10 min. There was a decrease in cell viability in the non-DPI-treated group exposed to LIPUS for

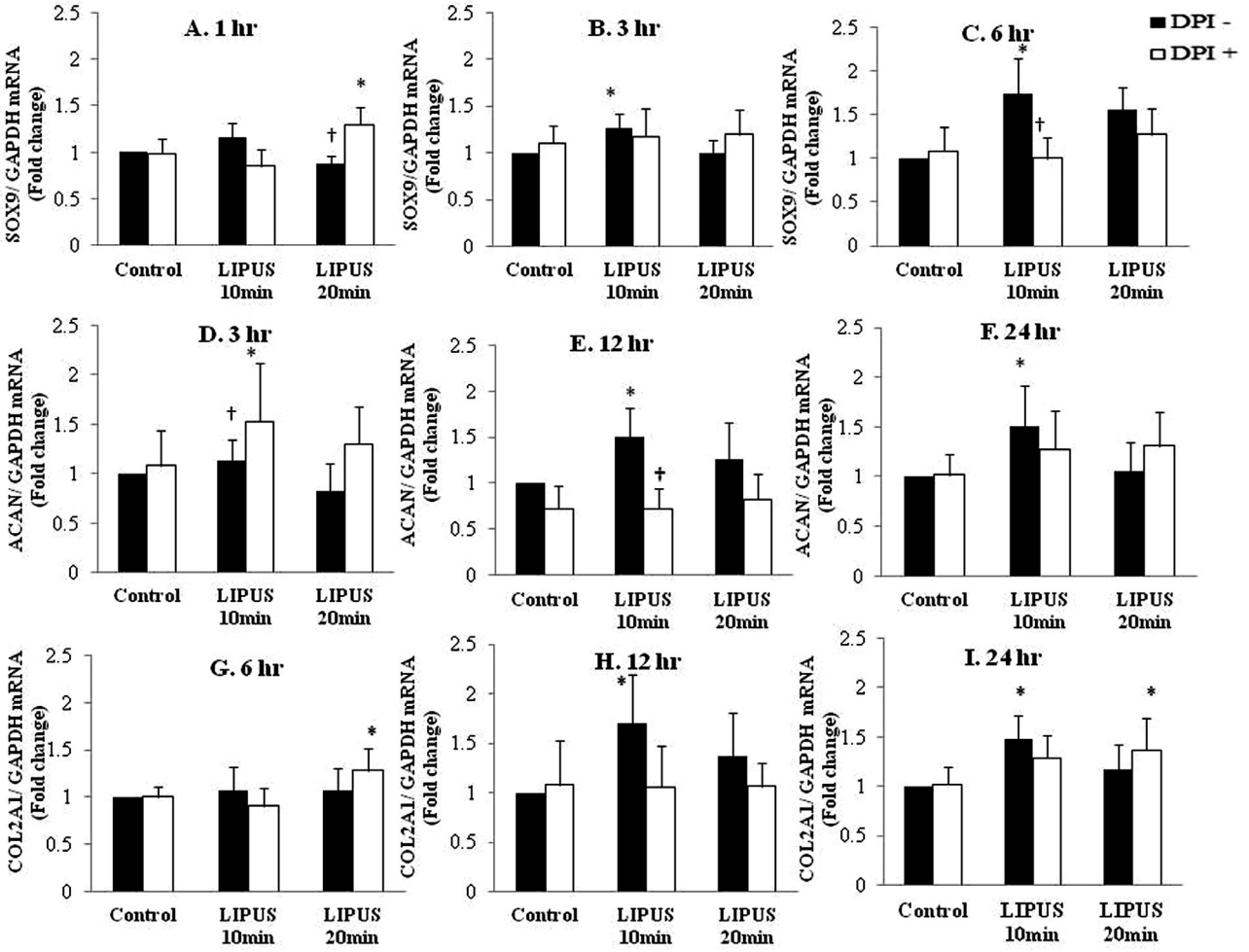

Fig. 4. Expression of *SOX9, ACAN* and *COL2* A1 mRNA quantified using quantitative real-time reverse transcription polymerase chain reaction in C28/I2 chondrocytes after LIPUS application in the presence or absence of DPI (10 μM). The samples were collected after (A) 1, (B) 3, (C) 6, (D) 12 and (E) 24 h of LIPUS. (A–C) Bar graphs reveal a significant increase in *SOX9* mRNA expression at 1, 3 and 6 h in the LIPUS-treated group compared with the control group. (D–F) Bar graphs reveal a significant increase in *ACAN* mRNA expression at 3, 12 and 24 h in the LIPUS-treated group compared with the control in non-DPI-treated groups. (G–I) Bar graphs depict a significant increase in COL2 A1 expression at 12 and 24 h in the LIPUS treated group compared with the control group in non-DPI-treated groups. *$p < 0.05$, $^{\dagger}p < 0.05$ between the corresponding DPI-treated and non-DPI-treated groups. DPI = diphenyleneiodonium; LIPUS = low-intensity pulsed ultrasound.

20 min. Similar results were seen in our previous studies in which exposure of pre-osteoblast cells to 20 min of LIPUS (Kaur et al. 2017b) and exposure of rat mandibular condyle to 40 min of LIPUS (Kaur et al. 2017a) decreased cell counts. This could be due to the thermal effect of LIPUS when applied for longer durations. Previous studies in *in vitro* (Leskinen and Hynynen 2012) and *in vivo* (Xue et al. 2013) setups also reported increases in temperature after 20 min of LIPUS. Future studies on the effects of LIPUS and ROS on cell proliferation are recommended. In DPI-treated groups, there was noteworthy difference in DPI-treated LIPUS-exposed groups at day 1 compared with non-DPI-treated groups. This could be due to a toxic effect of DPI. As mentioned earlier, DPI is a flavoprotein inhibitor and, most likely, caused inhibition of other enzymes like mitochondrial respiratory chain complex I (Majander et al. 1994), cholinesterase and the internal Ca^{2+} pump (Tazzeo and Janssen, 2009), flavin containing enzymes including nitric oxide synthase (Stuehr et al. 1991) and xanthine oxidase (Sanders et al. 1997), which are important for cell survival.

Sox9 is a transcription factor that regulates differentiation of stem cells toward chondrocytes and activates chondrocyte-specific markers like *COL2 A1* and *ACAN*. Sox9 binds to the enhancer element of the *Col II* gene and hence upregulates its expression (Oralová et al. 2015). Col II is the most abundant protein in the

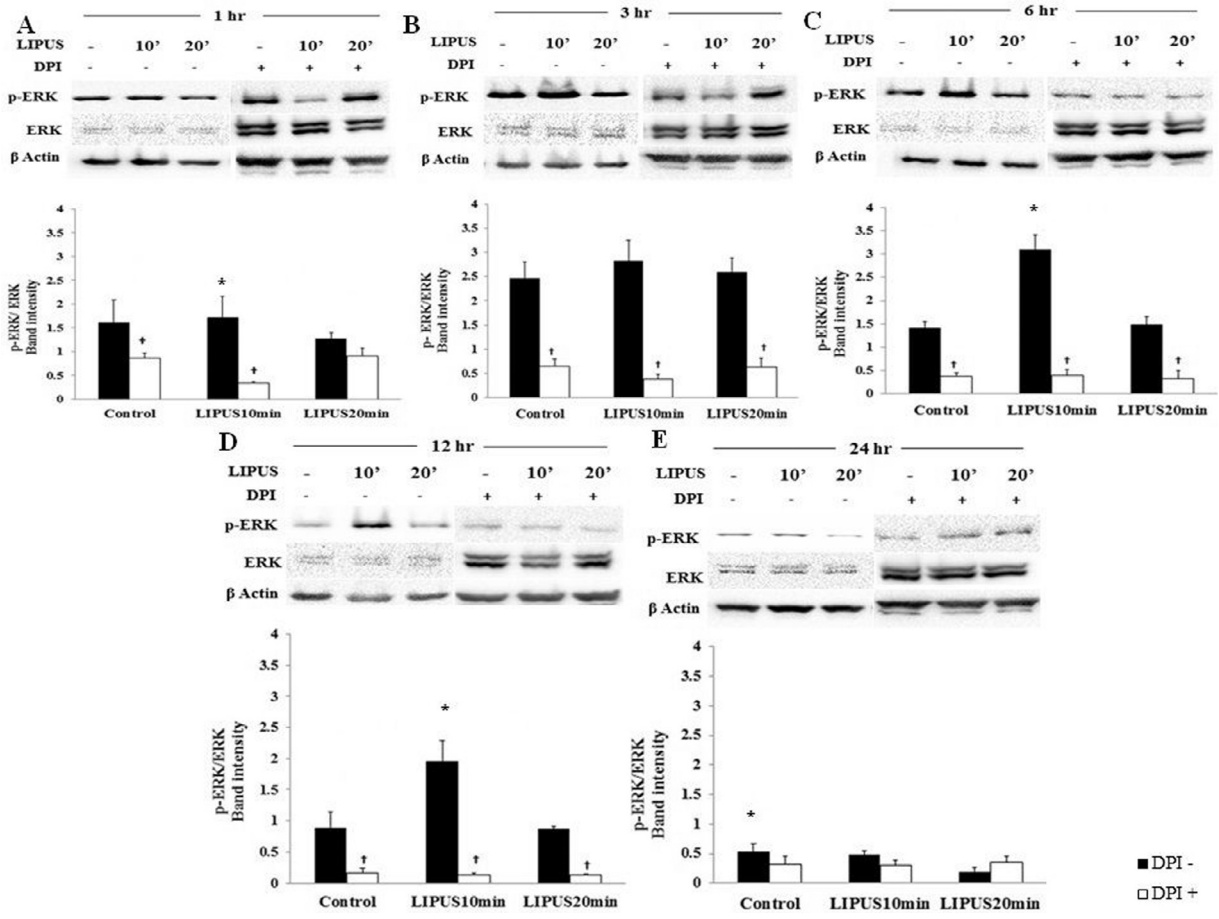

Fig. 5. Immunoblot analysis of ERK1/2 activation by LIPUS application. C28/I2 chondrocytes were treated with LIPUS in the presence or absence of DPI (10 μM). The samples were harvested for immunoblot analysis after (A) 1, (B) 3, (C) 6, (D) 12 and (E) 24 h of LIPUS. The phosphorylation level of ERK1/2 relative to total ERK1/2 was determined by the quantification of the band intensity using ImageJ software. LIPUS-treated groups exhibited a significant increase in the phosphorylation level at 6 and 12 h in the non-DPI-treated group; the phosphorylation level significantly decreased in the DPI-treated group. $^{*}p < 0.05$, $^{\dagger}p < 0.05$ between the corresponding DPI-treated and non-DPI-treated groups. DPI = diphenyleneiodonium; LIPUS = low-intensity pulsed ultrasound.

ECM of cartilage, and ACAN is a cartilage-specific proteoglycan core protein. These two components provide resistance against compressive loads and hence contribute to the viscoelastic properties of cartilage (Kuroda et al. 2009). Quantitative real-time reverse transcription polymerase chain reaction data from our study revealed a significant increase in mRNA expression of *SOX9* in the group exposed to LIPUS for 10 min, with the peak at 6 h. mRNA expression of *ACAN* and *COL2 A1* mRNA was also stimulated by 10 min of LIPUS in the absence of DPI at 12 h. There was a significant reduction in expression of *SOX9, ACAN* and *COL2 A1* in DPI-treated compared with non-DPI-treated groups. The previous study by Morita et al. (2007) indicated the role of ROS in chondrocyte differentiation in endochondral ossification both *in vitro* and *in vivo*. In that study, *N*-acetylcysteine (a ROS scavenger) inhibited chondrocyte hypertrophy in the ATDC5 chondrogenic cell line; similar results were seen when *N*-acetylcysteine was administered to normal mice. In our study we used an established chondrocyte cell line, C28/I2. Future studies with the ATDC5 chondrogenic cell line or primary bone marrow stem cells and LIPUS will be a good approach to studying the role of acoustically generated ROS in chondrocyte differentiation. We observed increased expression of *NOX2* in non-DPI-treated groups exposed to LIPUS for 10 min, whereas the *NOX4* expression level remained unchanged in DPI-treated and non-DPI-treated groups. An important feature of NOX4 is that it leads to the production of hydrogen peroxide (H_2O_2) directly in contrast to superoxide (Martyn et al. 2006). This also suggested that the ROS generated in our study was superoxide.

Finally, our study strongly indicated that superoxide plays an important role in MAPK signaling during

LIPUS application. In independent studies, LIPUS increased phosphorylation of MAPKs in osteoblasts, synovial cells, cementoblasts and chondrocytes (Ikeda et al. 2006). Our results also confirm the previous findings of these studies. Phosphorylation of ERK1/2 was significantly increased in LIPUS-exposed groups in the absence of DPI. Further, the phosphorylation level was significantly reduced in DPI-treated groups because of reduced ROS generation. In the case of p38 MAPK, the level of phosphorylation was increased in LIPUS-exposed, non-DPI-treated groups, but the difference was not significant. Interestingly, the suppression of ROS generation led to an increase in the phosphorylation level of JNK; however, the difference was not significant. MAPK activation leads to their translocation to the nucleus and increased phosphorylation of various intracellular molecules involved in cellular signaling, such as transcription factors, nuclear pore protein and cytoskeleton elements (Son et al. 2013). This study proves that the levels of phosphorylation of MAPKs are regulated by ROS generated during LIPUS application. ROS generated by LIPUS exposure has been revealed to be indispensable for intracellular signaling in chondrocytes.

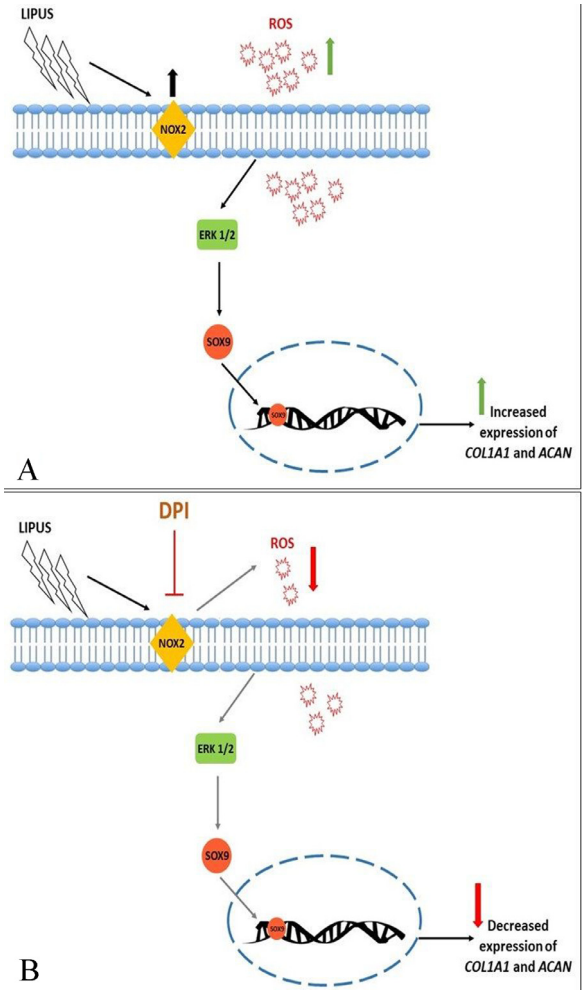

Fig. 6. Schematic of the effect of LIPUS on ROS expression in C28/I2 chondrocytes. (A) LIPUS increases the expression of *NOX2* and, thus, increases ROS in the cells. This leads to the activation and phosphorylation of ERK1/2 mitogen-activated protein kinase, which further increases *SOX9* expression. *SOX9* is the transcription factor for chondrogenic markers *ACAN* and *COL2 A1*. (B) DPI, on the other hand, inhibits *NOX2* and, hence, decreases ROS expression. This led to decreased phosphorylation of ERK1/2 mitogen-activated protein kinase and decreased expression of *SOX9, ACAN,* and *COL2 A1*. DPI = diphenyleneiodonium; LIPUS = low-intensity pulsed ultrasound; ROS = reactive oxygen species.

Since their initial discovery, ROS have been considered to cause deleterious effects in cells. In time, however, their role as intracellular secondary messengers has been recognized. These radicals play dual roles in cells as both injurious and positive signals, depending on the amount produced and the availability of cellular antioxidants (Bartosz 2009). Our study proved that superoxide produced by LIPUS exposure correlated with activation of MAPK pathways (ERK1/2 and p38) and hence increased gene expression of chondrocyte-specific markers (*SOX9, COL2 A1* and *ACAN*). Meanwhile, superoxide generation was downregulated by DPI, which was accompanied by inactivation of ERK and p38 and reduced expression of chondrocyte marker genes (Fig. 6).

CONCLUSIONS

Our study strongly suggests that the superoxide generated by LIPUS exposure leads to MAPK pathway activation in chondrocytes. Collectively, we conclude that ROS generated by LIPUS exposure play a key role in MAPK activation and matrix production.

Acknowledgments—This study was supported in part by the McIntyre Fund, Division of Orthodontics, Department of Dentistry, Faculty of Medicine and Dentistry, University of Alberta, and Dr. Hasan Uludag, Department of Biomedical Engineering, Department of Chemical and Material Engineering, University of Alberta.

SUPPLEMENTARY MATERIALS

Supplementary material associated with this article can be found, in the online version, at doi:10.1016/j.ultrasmedbio.2018.05.025.

REFERENCES

Bartosz G. Reactive oxygen species: destroyers or messengers?. Biochem Pharmacol 2009;77:1303–1315.

Boutros T, Chevet E, Metrakos P. Mitogen-activated protein (MAP) kinase/MAP kinase phosphatase regulation: Roles in cell growth, death, and cancer. Pharmacol Rev 2008;60:261–310.

Busse JW, Kaur J, Mollon B, Bhandari M, Tornetta III P, Schünemann HJ, Guyatt GH. Low intensity pulsed ultrasonography for fractures: Systematic review of randomised controlled trials. BMJ 2009;338:b351.

Cheng K, Xia P, Lin Q, Shen S, Gao M, Ren S, Li X. Effects of low-intensity pulsed ultrasound on integrin-FAK-PI3 K/Akt mechanochemical transduction in rabbit osteoarthritis chondrocytes. Ultrasound Med Biol 2014;40:1609–1618.

Cheung WH, Chow SK, Sun MH, Qin L, Leung KS. Low-intensity pulsed ultrasound accelerated callus formation, angiogenesis and callus remodeling in osteoporotic fracture healing. Ultrasound Med Biol 2011;37:231–238.

Choi BH, Choi MH, Kwak MG, Min BH, Woo ZH, Park SR. Mechanotransduction pathways of low-intensity ultrasound in C-28/I2 human chondrocyte cell line. J Eng Med 2007;221:527–535.

El-Bialy T, Uludag H, Jomha N, Badylak SF. In vivo ultrasound-assisted tissue-engineered mandibular condyle: A pilot study in rabbits. Tissue Eng 2010;16:1315–1323.

Fanghänel J, Gedrange T. On the development, morphology and function of the temporomandibular joint in the light of the orofacial system. Ann Anat 2007;189:314–319.

Fujisawa T, Takeda K, Ichijo H. ASK family proteins in stress response and disease. Mol Biotechnol 2007;37:13–18.

Hasanova GI, Noriega SE, Mamedov TG, Thakurta SG, Turner JA, Subramanian A. The effect of ultrasound stimulation on the gene and protein expression of chondrocytes seeded in chitosan scaffolds. J Tissue Eng Regen Med 2011;5:815–822.

Hsu S, Huang T. Bioeffect of ultrasound on endothelial cells in vitro. Biomol Eng 2004;21:99–104.

Ikeda K, Takayama T, Suzuki N, Shimada K, Otsuka K, Ito K. Effects of low-intensity pulsed ultrasound on the differentiation of C2 C12 cells. Life Sci 2006;79:1936–1943.

Jortikka MO, Inkinen RI, Tammi MI, Parkkinen JJ, Haapala J, Kiviranta I, Helminen HJ, Lammi MJ. Immobilisation causes longlasting matrix changes both in the immobilized and contralateral joint cartilage. Ann Rheum Dis 1997;56:255–261.

Kaur H, Uludağ H, Dederich DN, El-Bialy T. Effect of increasing low-intensity pulsed ultrasound and a functional appliance on the mandibular condyle in growing rats. J Ultrasound Med 2017;36:109–120.

Kaur H, Siraki AG, Uludağ H, Dederich DN, Flood P, El-Bialy T. Role of reactive oxygen species during low-intensity pulsed ultrasound application in MC-3 T3 E1 pre-osteoblast cell culture. Ultrasound Med Biol 2017;43:2699–2712.

Kuroda S, Tanimoto K, Izawa T, Fujihara S, Koolstra JH, Tanaka E. Biomechanical and biochemical characteristics of the mandibular condylar cartilage. Osteoarthritis Cartilage 2009;17:1408–1415.

Kusuyama J, Bandow K, Shamoto M, Kakimoto K, Ohnishi T, Matsuguchi T. Low intensity pulsed ultrasound (LIPUS) influences the multilineage differentiation of mesenchymal stem and progenitor cell lines through ROCK-Cot/Tpl2-MEK-ERK signaling pathway. J Biol Chem 2014;289:10330–10344.

Leskinen JJ, Hynynen K. Study of factors affecting the magnitude and nature of ultrasound exposure with in vitro set-ups. Ultrasound Med Biol 2012;38:777–794.

Li N, Ragheb K, Lawler G, Sturgis J, Rajwa B, Melendez JA, Robinson JP. DPI induces mitochondrial superoxide-mediated apoptosis. Free Radical Biol Med 2003;34:465–477.

Majander A, Finel M, Wikström M. Diphenyleneiodonium inhibits reduction of iron−sulfur clusters in the mitochondrial NADH−ubiquinone oxidoreductase (complex I). J Biol Chem 1994;269:21037–21042.

Martyn KD, Frederick LM, von Loehneysen K, Dinauer MC, Knaus UG. Functional analysis of Nox4 reveals unique characteristics compared to other NADPH oxidases. Cell Signal 2006;18:69–82.

Morita K, Miyamoto T, Fujita N, Kubota Y, Ito K, Takubo K, Miyamoto K, Ninomiya K, Suzuki T, Iwasaki R, Yagi M, Takaishi H, Toyama Y, Suda T. Reactive oxygen species induce chondrocyte hypertrophy in endochondral ossification. J Exp Med 2007;204:1613–1623.

Mortimer AJ, Dyson M. The effect of therapeutic ultrasound on calcium uptake in fibroblasts. Ultrasound Med Biol 1988;14:499–506.

Oralová V, Matalová E, Janečková E, Krejčí ED, Knopfová L, Šnajdr P, Tucker AS, Veselá I, Šmarda J, Buchtová M. Role of c-myb in chondrogenesis. Bone 2015;76:97–106.

Peshavariya HM, Dusting GJ, Selemidis S. Analysis of dihydroethidium fluorescence for the detection of intracellular and extracellular superoxide produced by NADPH oxidase. Free Radical Res 2007;41:699–712.

Plotnikov A, Zehorai E, Procaccia S, Seger R. The MAPK cascades: signaling components, nuclear roles and mechanisms of nuclear translocation. Biochim Biophys Acta 2011;1813:1619–1633.

Reher PMH, Whiteman M, Hai HK, Meghji S. Ultrasound stimulates nitric oxide and prostaglandin e_2 production by human osteoblasts. Bone 2002;31:236–241.

Sanders SA, Eisenthal R, Harrison R. NADH oxidase activity of human xanthine oxidoreductase-generation of superoxide anion. Eur J Biochem 1997;245:541–548.

Sato H, Kawamura A, Yamaguchi M, Kasai K. Relationship between masticatory function and internal structure of the mandible based on computed tomography findings. Am J Orthod Dentofacial Orthoped 2005;128:766–773.

Sato M, Nagata K, Kuroda S, Horiuchi S, Nakamura T, Karima M, Inubushi T, Tanaka E. Low-intensity pulsed ultrasound activates integrin-mediated mechanotransduction pathway in synovial cells. Ann Biomed Eng 2014;42:2156–2163.

Sauer H, Wartenberg M, Hescheler J. Reactive oxygen species as intracellular messengers during cell growth and differentiation. Cell Physiol Biochem 2001;11:173–186.

Son Y, Kim S, Chung HT, Pae HO. Reactive oxygen species in the activation of MAP Kinases. In: Cadenas E, Packer L, (eds). Methods in enzymology. New York: Academic Press; 2013. p. 27–48.

Stuehr DJ, Fasehun OA, Kwon NS, Gross SS, Gonzalez JA, Levi R, Nathan CF. Inhibition of macrophage and endothelial cell nitric oxide synthase by diphenyleneiodonium and its analogs. FASEB J 1991;5:98–103.

Takeuchi R, Ryo A, Komitsu N, Takagaki YM, Fukui A, Takagi Y, Shiraishi T, Morishita S, Yamazaki Y, Kumagai K, Aoki I, Saito T. Low-intensity pulsed ultrasound activates the phosphatidylinositol 3 kinase/Akt pathway and stimulates the growth of chondrocytes in three-dimensional cultures: A basic science study. Arthritis Res Ther 2008;10:R77.

Tanaka E, Kuroda S, Horiuchi S, Tabata A, El-Bialy T. Low-intensity pulsed ultrasound in dentofacial tissue engineering. Ann Biomed Eng 2015;43:871–886.

Tazzeo TF W, Janssen LJ. The NADPH oxidase inhibitor diphenyleneiodonium is also a potent inhibitor of cholinesterases and the internal Ca^{2+} pump. Br J Pharmacol 2009;158:790–796.

Uddin SMZ, Hadjiargyrou M, Cheng J, Zhang S, Hu M, Qin YX. Reversal of the detrimental effects of simulated microgravity on human osteoblasts by modified low intensity pulsed ultrasound. Ultrasound Med Biol 2013;39:804–812.

Whitney NP, Lamb AC, Louw TM, Subramanian A. Integrin mediated mechanotransduction pathway of low intensity continuous ultrasound in human chondrocytes. Ultrasound Med Biol 2012;38:1734–1743.

Xue H, Zheng J, Cui Z, Bai X, Li G, Zhang C, He S, Li W, Lajud SA, Duan Y, Zhou H. Low intensity pulsed ultrasound accelerates tooth movement via activation of the BMP-2 signaling pathway. PloS One 2013;8:e68926.